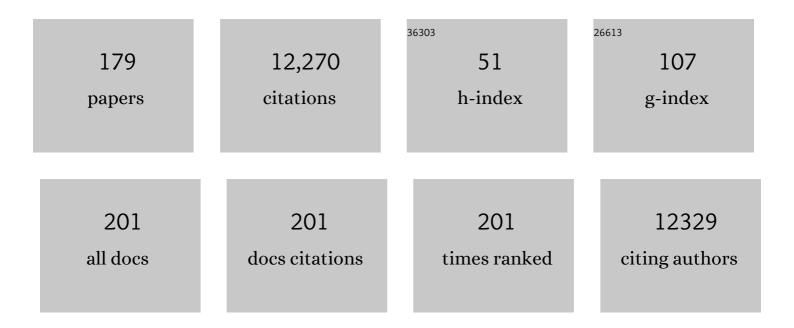
List of Publications by Year in descending order

Source: https://exaly.com/author-pdf/10198139/publications.pdf Version: 2024-02-01



AMRDOS I REED

#	Article	IF	CITATIONS
1	Evaluation of Hybrid ⁶⁸ Ga-PSMA Ligand PET/CT in 248 Patients with Biochemical Recurrence After Radical Prostatectomy. Journal of Nuclear Medicine, 2015, 56, 668-674.	5.0	907
2	Imaging biomarker roadmap for cancer studies. Nature Reviews Clinical Oncology, 2017, 14, 169-186.	27.6	792
3	Diagnostic Efficacy of ⁶⁸ Gallium-PSMA Positron Emission Tomography Compared to Conventional Imaging for Lymph Node Staging of 130 Consecutive Patients with Intermediate to High Risk Prostate Cancer. Journal of Urology, 2016, 195, 1436-1443.	0.4	659
4	First Clinical Experience with Integrated Whole-Body PET/MR: Comparison to PET/CT in Patients with Oncologic Diagnoses. Journal of Nuclear Medicine, 2012, 53, 845-855.	5.0	466
5	Simultaneous 68Ga-PSMA HBED-CC PET/MRI Improves the Localization of Primary Prostate Cancer. European Urology, 2016, 70, 829-836.	1.9	456
6	Time Course of Tumor Metabolic Activity During Chemoradiotherapy of Esophageal Squamous Cell Carcinoma and Response to Treatment. Journal of Clinical Oncology, 2004, 22, 900-908.	1.6	448
7	Noninvasive Visualization of the Activated $\hat{1}\pm v\hat{1}^2$ 3 Integrin in Cancer Patients by Positron Emission Tomography and [18F]Galacto-RGD. PLoS Medicine, 2005, 2, e70.	8.4	443
8	Positron Emission Tomography Using [18F]Galacto-RGD Identifies the Level of Integrin αvβ3 Expression in Man. Clinical Cancer Research, 2006, 12, 3942-3949.	7.0	337
9	SPECT/CT. Journal of Nuclear Medicine, 2008, 49, 1305-1319.	5.0	280
10	[18F]Galacto-RGD Positron Emission Tomography for Imaging of αvβ3 Expression on the Neovasculature in Patients with Squamous Cell Carcinoma of the Head and Neck. Clinical Cancer Research, 2007, 13, 6610-6616.	7.0	217
11	Value of ⁶⁸ Ga-PSMA HBED-CC PET for the Assessment of Lymph Node Metastases in Prostate Cancer Patients with Biochemical Recurrence: Comparison with Histopathology After Salvage Lymphadenectomy. Journal of Nuclear Medicine, 2016, 57, 1713-1719.	5.0	213
12	Imaging of integrin $\hat{I} \pm v \hat{I}^2 3$ expression. Cancer and Metastasis Reviews, 2008, 27, 631-644.	5.9	208
13	Radiolabelled RGD peptides for imaging and therapy. European Journal of Nuclear Medicine and Molecular Imaging, 2012, 39, 126-138.	6.4	203
14	Biodistribution and pharmacokinetics of the alphavbeta3-selective tracer 18F-galacto-RGD in cancer patients. Journal of Nuclear Medicine, 2005, 46, 1333-41.	5.0	202
15	Observation of the Swallowing Process by Application of Videofluoroscopy and Real-time Magnetic Resonance ImagingConsequences for Retronasal Aroma Stimulation. Chemical Senses, 2001, 26, 1211-1219.	2.0	192
16	lmaging of integrin αvβ3 expression in patients with malignant glioma by [18F] Galacto-RGD positron emission tomography. Neuro-Oncology, 2009, 11, 861-870.	1.2	180
17	<i>In vivo</i> molecular imaging of chemokine receptor <scp>CXCR</scp> 4 expression in patients with advanced multiple myeloma. EMBO Molecular Medicine, 2015, 7, 477-487.	6.9	180
18	Comparison of Integrin α _v β ₃ Expression and Glucose Metabolism in Primary and Metastatic Lesions in Cancer Patients: A PET Study Using ¹⁸ F-Galacto-RGD and ¹⁸ F-FDG. Journal of Nuclear Medicine, 2008, 49, 22-29.	5.0	173

#	Article	IF	CITATIONS
19	Patterns of α _v l² ₃ Expression in Primary and Metastatic Human Breast Cancer as Shown by ¹⁸ F-Galacto-RGD PET. Journal of Nuclear Medicine, 2008, 49, 255-259.	5.0	170
20	Disclosing the CXCR4 Expression in Lymphoproliferative Diseases by Targeted Molecular Imaging. Theranostics, 2015, 5, 618-630.	10.0	162
21	Expression of Integrin α _v β ₃ in Gliomas Correlates with Tumor Grade and Is not Restricted to Tumor Vasculature. Brain Pathology, 2008, 18, 378-386.	4.1	161
22	Value of a Dixon-based MR/PET attenuation correction sequence for the localization and evaluation of PET-positive lesions. European Journal of Nuclear Medicine and Molecular Imaging, 2011, 38, 1691-1701.	6.4	161
23	Diffusionâ€weighted imaging outside the brain: Consensus statement from an ISMRMâ€sponsored workshop. Journal of Magnetic Resonance Imaging, 2016, 44, 521-540.	3.4	146
24	PET/CT Imaging of Integrin αvβ3 Expression in Human Carotid Atherosclerosis. JACC: Cardiovascular Imaging, 2014, 7, 178-187.	5.3	145
25	Preliminary Results for Characterization of Pelvic Lymph Nodes in Patients With Prostate Cancer by Diffusion-Weighted MR-Imaging. Investigative Radiology, 2010, 45, 15-23.	6.2	143
26	Performance of Whole-Body Integrated ¹⁸ F-FDG PET/MR in Comparison to PET/CT for Evaluation of Malignant Bone Lesions. Journal of Nuclear Medicine, 2014, 55, 191-197.	5.0	134
27	PET Imaging of Integrin $\hat{I}\pm V\hat{I}^2$ 3 Expression. Theranostics, 2011, 1, 48-57.	10.0	117
28	High-resolution MRI vs multislice spiral CT: Which technique depicts the trabecular bone structure best?. European Radiology, 2003, 13, 663-671.	4.5	114
29	PET/MR Imaging in the Detection and Characterization of Pulmonary Lesions: Technical and Diagnostic Evaluation in Comparison to PET/CT. Journal of Nuclear Medicine, 2014, 55, 724-729.	5.0	113
30	Physiological and analytical studies on flavor perception dynamics as induced by the eating and swallowing process. Food Quality and Preference, 2002, 13, 497-504.	4.6	109
31	Workflow and Scan Protocol Considerations for Integrated Whole-Body PET/MRI in Oncology. Journal of Nuclear Medicine, 2012, 53, 1415-1426.	5.0	109
32	PET-based human dosimetry of 18F-galacto-RGD, a new radiotracer for imaging alpha v beta3 expression. Journal of Nuclear Medicine, 2006, 47, 763-9.	5.0	109
33	Comparison of integrated whole-body [11C]choline PET/MR with PET/CT in patients with prostate cancer. European Journal of Nuclear Medicine and Molecular Imaging, 2013, 40, 1486-1499.	6.4	107
34	Pittsburgh compound B imaging and cerebrospinal fluid amyloid-β in a multicentre European memory clinic study. Brain, 2016, 139, 2540-2553.	7.6	107
35	Positron emission tomography tracers for imaging angiogenesis. European Journal of Nuclear Medicine and Molecular Imaging, 2010, 37, 86-103.	6.4	102
36	Radionuclide and hybrid imaging of recurrent prostate cancer. Lancet Oncology, The, 2011, 12, 181-191.	10.7	94

#	Article	IF	CITATIONS
37	68Ga-NODAGA-RGD is a suitable substitute for 18F-Galacto-RGD and can be produced with high specific activity in a cGMP/GRP compliant automated process. Nuclear Medicine and Biology, 2012, 39, 777-784.	0.6	93
38	Wholeâ€body MRI including diffusionâ€weighted imaging (DWI) for patients with recurring prostate cancer: Technical feasibility and assessment of lesion conspicuity in DWI. Journal of Magnetic Resonance Imaging, 2011, 33, 1160-1170.	3.4	83
39	Adenocarcinomas of Esophagogastric Junction: Multi–Detector Row CT to Evaluate Early Response to Neoadjuvant Chemotherapy. Radiology, 2006, 239, 472-480.	7.3	81
40	Reliability of MR Imaging—Based Virtual Cystoscopy in the Diagnosis of Cancer of the Urinary Bladder. American Journal of Roentgenology, 2002, 178, 1483-1488.	2.2	80
41	Potential clinical implications of <i>BRAF</i> mutations in histiocytic proliferations. Oncotarget, 2014, 5, 4060-4070.	1.8	78
42	Application of RGD-containing peptides as imaging probes for alphavbeta3 expression. Frontiers in Bioscience - Landmark, 2009, Volume, 887.	3.0	69
43	PET-MRI Fusion in Head-and-Neck Oncology: Current Status and Implications for Hybrid PET/MRI. Journal of Oral and Maxillofacial Surgery, 2012, 70, 473-483.	1.2	69
44	Rectal Cancer: MR Imaging before Neoadjuvant Chemotherapy and Radiation Therapy for Prediction of Tumor-Free Circumferential Resection Margins and Long-term Survival1. Radiology, 2007, 243, 744-751.	7.3	63
45	Diagnostic value of MRI-based 3D texture analysis for tissue characterisation and discrimination of low-grade chondrosarcoma from enchondroma: a pilot study. European Radiology, 2018, 28, 468-477.	4.5	62
46	Restricted Water Diffusibility as Measured by Diffusion-weighted MR Imaging and Choline Uptake in 11C-Choline PET/CT are Correlated in Pelvic Lymph Nodes in Patients with Prostate Cancer. Molecular Imaging and Biology, 2011, 13, 352-361.	2.6	61
47	Combined PET/MRI: Multi-modality Multi-parametric Imaging Is Here. Molecular Imaging and Biology, 2015, 17, 595-608.	2.6	56
48	Magnetic resonance imaging of myocardial injury and ventricular torsion after marathon running. Clinical Science, 2011, 120, 143-152.	4.3	55
49	Evaluation of Feasibility and Image Quality of 68Ga-DOTATOC Positron Emission Tomography/Magnetic Resonance in Comparison With Positron Emission Tomography/Computed Tomography in Patients With Neuroendocrine Tumors. Investigative Radiology, 2013, 48, 263-272.	6.2	55
50	The Effect of Total Tumor Volume on the Biologically Effective Dose to Tumor and Kidneys for ¹⁷⁷ Lu-Labeled PSMA Peptides. Journal of Nuclear Medicine, 2018, 59, 929-933.	5.0	54
51	Dynamics of retronasal aroma perception during consumption: Cross-linking on-line breath analysis with medico-analytical tools to elucidate a complex process. Food Chemistry, 2008, 108, 1234-1246.	8.2	51
52	Comparison of 3′-deoxy-3′-[18F]fluorothymidine positron emission tomography (FLT PET) and FDG PET/CT for the detection and characterization of pancreatic tumours. European Journal of Nuclear Medicine and Molecular Imaging, 2012, 39, 846-851.	6.4	51
53	Dynamic near-real-time magnetic resonance imaging for analyzing the velopharyngeal closure in comparison with videofluoroscopy. Journal of Magnetic Resonance Imaging, 2004, 20, 791-797.	3.4	49
54	PET/MR in prostate cancer: technical aspects and potential diagnostic value. European Journal of Nuclear Medicine and Molecular Imaging, 2013, 40, 79-88.	6.4	49

#	Article	IF	CITATIONS
55	Systematic Comparison of the Performance of Integrated Whole-Body PET/MR Imaging to Conventional PET/CT for ¹⁸ F-FDG Brain Imaging in Patients Examined for Suspected Dementia. Journal of Nuclear Medicine, 2014, 55, 923-931.	5.0	46
56	lmaging of Tumor Angiogenesis for Radiologists—Part 1: Biological and Technical Basis. Current Problems in Diagnostic Radiology, 2015, 44, 407-424.	1.4	45
57	Discrimination Between Brown and White Adipose Tissue Using a 2-Point Dixon Water–Fat Separation Method in Simultaneous PET/MRI. Journal of Nuclear Medicine, 2015, 56, 1742-1747.	5.0	45
58	Intrapatient Comparison of 111In-PSMA I&T SPECT/CT and Hybrid 68Ga-HBED-CC PSMA PET in Patients With Early Recurrent Prostate Cancer. Clinical Nuclear Medicine, 2016, 41, e397-e402.	1.3	45
59	Optimized Peptide Amount and Activity for ⁹⁰ Y-Labeled DOTATATE Therapy. Journal of Nuclear Medicine, 2016, 57, 503-508.	5.0	45
60	¹⁸ Fâ€Fluorodeoxyglucose positron emission tomography/computed tomography for the detection of recurrent bone and soft tissue sarcoma. Cancer, 2013, 119, 1227-1234.	4.1	44
61	Radiofluorination of PSMA-HBED via Al18F2+ Chelation and Biological Evaluations In Vitro. Molecular Imaging and Biology, 2015, 17, 777-785.	2.6	44
62	Selective Imaging of the Angiogenic Relevant Integrins α5β1 and αvβ3. Angewandte Chemie - International Edition, 2013, 52, 11656-11659.	13.8	43
63	Multimodal Molecular Imaging of Integrin α _v l² ₃ for In Vivo Detection of Pancreatic Cancer. Journal of Nuclear Medicine, 2014, 55, 446-451.	5.0	43
64	Preoperative lymph node staging in patients with primary prostate cancer: comparison and correlation of quantitative imaging parameters in diffusion-weighted imaging and 11C-choline PET/CT. European Radiology, 2014, 24, 1821-1826.	4.5	41
65	Modeling and Predicting Tumor Response in Radioligand Therapy. Journal of Nuclear Medicine, 2019, 60, 65-70.	5.0	41
66	Phenotyping of Tumor Biology in Patients by Multimodality Multiparametric Imaging: Relationship of Microcirculation, αvβ3 Expression, and Glucose Metabolism. Journal of Nuclear Medicine, 2010, 51, 1691-1698.	5.0	39
67	Comparison of 16-MDCT and MRI for Characterization of Kidney Lesions. American Journal of Roentgenology, 2006, 186, 1639-1650.	2.2	38
68	Ferumoxtran-10-enhanced MR imaging of the bone marrow before and after conditioning therapy in patients with non-Hodgkin lymphomas. European Radiology, 2006, 16, 598-607.	4.5	38
69	Characterization of carotid artery plaques with USPIO-enhanced MRI: assessment of inflammation and vascularity as in vivo imaging biomarkers for plaque vulnerability. International Journal of Cardiovascular Imaging, 2011, 27, 901-912.	1.5	37
70	Quantitative and correlative biodistribution analysis of ⁸⁹ Zr-labeled mesoporous silica nanoparticles intravenously injected into tumor-bearing mice. Nanoscale, 2017, 9, 9743-9753.	5.6	35
71	Prospective head-to-head comparison of 11C-choline-PET/MR and 11C-choline-PET/CT for restaging of biochemical recurrent prostate cancer. European Journal of Nuclear Medicine and Molecular Imaging, 2017, 44, 2179-2188.	6.4	35
72	MR cystography for bladder tumor detection. European Radiology, 2004, 14, 2311-2319.	4.5	32

#	Article	IF	CITATIONS
73	Simulation of a MR–PET protocol for staging of head-and-neck cancer including Dixon MR for attenuation correction. European Journal of Radiology, 2012, 81, 2658-2665.	2.6	31
74	ls Câ€11ÂMethionine PET/CT Able to Localise Sestamibiâ€Negative Parathyroid Adenomas?. World Journal of Surgery, 2017, 41, 980-985.	1.6	31
75	Rectal Carcinoma: High-Spatial-Resolution MR Imaging and T2 Quantification in Rectal Cancer Specimens. Radiology, 2006, 241, 132-141.	7.3	30
76	Investigating the Effect of Ligand Amount and Injected Therapeutic Activity: A Simulation Study for 177Lu-Labeled PSMA-Targeting Peptides. PLoS ONE, 2016, 11, e0162303.	2.5	30
77	Diagnostic value of retrospective PET-MRI fusion in head-and-neck cancer. BMC Cancer, 2014, 14, 846.	2.6	29
78	Multiparametric MR and PET Imaging of Intratumoral Biological Heterogeneity in Patients with Metastatic Lung Cancer Using Voxel-by-Voxel Analysis. PLoS ONE, 2015, 10, e0132386.	2.5	28
79	FDG-PET underscores the key role of the thalamus in frontotemporal lobar degeneration caused by C9ORF72 mutations. Translational Psychiatry, 2019, 9, 54.	4.8	28
80	The effect of ligand amount, affinity and internalization on PSMA-targeted imaging and therapy: A simulation study using a PBPK model. Scientific Reports, 2019, 9, 20041.	3.3	28
81	Influence of sampling schedules on [177Lu]Lu-PSMA dosimetry. EJNMMI Physics, 2020, 7, 41.	2.7	27
82	Apparent Diffusion Coefficient (ADC) predicts therapy response in pancreatic ductal adenocarcinoma. Scientific Reports, 2017, 7, 17038.	3.3	26
83	Interobserver variability, detection rate, and lesion patterns of 68Ga-PSMA-11-PET/CT in early-stage biochemical recurrence of prostate cancer after radical prostatectomy. European Journal of Nuclear Medicine and Molecular Imaging, 2020, 47, 2339-2347.	6.4	26
84	Evaluation of ¹⁸ F-Fluoride PET/MR and PET/CT in Patients with Foot Pain of Unclear Cause. Journal of Nuclear Medicine, 2015, 56, 430-435.	5.0	25
85	11C-choline PET/CT and whole-body MRI including diffusion-weighted imaging for patients with recurrent prostate cancer. Oncotarget, 2017, 8, 66516-66527.	1.8	25
86	Prospective study on bright lumen magnetic resonance colonography in comparison with conventional colonoscopy. British Journal of Radiology, 2007, 80, 235-241.	2.2	24
87	Bone mineral density measurements of the proximal femur from routine contrast-enhanced MDCT data sets correlate with dual-energy X-ray absorptiometry. European Radiology, 2013, 23, 505-512.	4.5	24
88	Multiparametric PET and MRI of myocardial damage after myocardial infarction: correlation of integrin αvβ3 expression and myocardial blood flow. European Journal of Nuclear Medicine and Molecular Imaging, 2021, 48, 1070-1080.	6.4	24
89	Non-invasive tracking of human haemopoietic CD34+ stem cells in vivo in immunodeficient mice by using magnetic resonance imaging. European Radiology, 2010, 20, 2184-2193.	4.5	23
90	Positron emission tomography/magnetic resonance imaging with ⁶⁸ <scp>G</scp> alliumâ€labeled ligand of prostateâ€specific membrane antigen: Promising novel option in prostate cancer imaging?. International Journal of Urology, 2014, 21, 1286-1288.	1.0	23

#	Article	IF	CITATIONS
91	Prognostic value of [18F]FDG-PET/CT in multiple myeloma patients before and after allogeneic hematopoietic cell transplantation. European Journal of Nuclear Medicine and Molecular Imaging, 2018, 45, 1694-1704.	6.4	23
92	PET Imaging of αvβ3 Expression in Cancer Patients. Methods in Molecular Biology, 2011, 680, 183-200.	0.9	23
93	Visualization of stress fractures of the foot using PET-MRI: a feasibility study. European Journal of Medical Research, 2015, 20, 99.	2.2	22
94	In vivo biokinetic and metabolic characterization of the 68Ga-labelled α5β1-selective peptidomimetic FR366. European Journal of Nuclear Medicine and Molecular Imaging, 2016, 43, 953-963.	6.4	22
95	PET imaging of gliomas using novel tracers: a sleeping beauty waiting to be kissed. Expert Review of Anticancer Therapy, 2010, 10, 609-613.	2.4	21
96	Tumors of the urinary bladder: technique, current use, and perspectives of MR and CT cystography. Abdominal Imaging, 2003, 28, 868-76.	2.0	20
97	Physiologically Based Pharmacokinetic Modeling Is Essential in 90Y-Labeled Anti-CD66 Radioimmunotherapy. PLoS ONE, 2015, 10, e0127934.	2.5	20
98	Assessment of Tumor Volumes in Skull Base Glomus Tumors Using Gluc-Lys[18F]-TOCA Positron Emission Tomography. International Journal of Radiation Oncology Biology Physics, 2009, 73, 1135-1140.	0.8	19
99	Prognostic Value of ¹¹ C-Choline PET/CT and CT for Predicting Survival of Bladder Cancer Patients Treated with Radical Cystectomy. Urologia Internationalis, 2014, 93, 207-213.	1.3	19
100	Multi-Modal PET and MR Imaging in the Hen's Egg Test-Chorioallantoic Membrane (HET-CAM) Model for Initial In Vivo Testing of Target-Specific Radioligands. Cancers, 2020, 12, 1248.	3.7	18
101	Non-invasive assessment of inter-and intrapatient variability of integrin expression in metastasized prostate cancer by PET. Oncotarget, 2016, 7, 28151-28159.	1.8	18
102	Recommendations for measurement of tumour vascularity with positron emission tomography in early phase clinical trials. European Radiology, 2012, 22, 1465-1478.	4.5	17
103	Comparative Oncology: Evaluation of 2-Deoxy-2-[18F]fluoro-D-glucose (FDG) Positron Emission Tomography/Computed Tomography (PET/CT) for the Staging of Dogs with Malignant Tumors. PLoS ONE, 2015, 10, e0127800.	2.5	17
104	Microtiter plate-based antibody-competition assay to determine binding affinities and plasma/blood stability of CXCR4 ligands. Scientific Reports, 2020, 10, 16036.	3.3	17
105	PET/CT with Gluc-Lys-([18F]FP)-TOCA: correlation between uptake, size and arterial perfusion in somatostatin receptor positive lesions. European Journal of Nuclear Medicine and Molecular Imaging, 2008, 35, 264-271.	6.4	16
106	Visualization of antigen-specific human cytotoxic T lymphocytes labeled with superparamagnetic iron-oxide particles. European Radiology, 2008, 18, 1087-1095.	4.5	16
107	Value of PET imaging for radiation therapy. Strahlentherapie Und Onkologie, 2021, 197, 1-23.	2.0	16
108	PET/MR imaging of atherosclerosis: initial experience and outlook. American Journal of Nuclear Medicine and Molecular Imaging, 2013, 3, 393-6.	1.0	16

#	Article	IF	CITATIONS
109	PET/MR in Oncology: Non–18F-FDG Tracers for Routine Applications. Journal of Nuclear Medicine, 2014, 55, 25S-31S.	5.0	15
110	Imaging of Tumor Angiogenesis for Radiologists—Part 2: Clinical Utility. Current Problems in Diagnostic Radiology, 2015, 44, 425-436.	1.4	15
111	Treatment planning algorithm for peptide receptor radionuclide therapy considering multiple tumor lesions and organs at risk. Medical Physics, 2018, 45, 3516-3523.	3.0	15
112	First experiences with Lu-177 PSMA therapy in combination with Pembrolizumab or after pretreatment with Olaparib in single patients. Journal of Nuclear Medicine, 2021, 62, jnumed.120.249029.	5.0	15
113	PET of αvβ3-Integrin and αvβ5-Integrin Expression with 18F-Fluciclatide for Assessment of Response to Targeted Therapy: Ready for Prime Time?. Journal of Nuclear Medicine, 2011, 52, 335-337.	5.0	14
114	Sensitivity of PET/MRI to detect recurrence of prostate cancer. European Journal of Nuclear Medicine and Molecular Imaging, 2013, 40, 799-799.	6.4	14
115	Simple liver cysts and cystoid lesions in hepatic alveolar echinococcosis: a retrospective cohort study with Hounsfield analysis. Parasite, 2019, 26, 54.	2.0	14
116	Hepatic alveolar echinococcosis: correlation between computed tomography morphology and inflammatory activity in positron emission tomography. Scientific Reports, 2020, 10, 11808.	3.3	14
117	In vivo PET/MRI Imaging of the Chorioallantoic Membrane. Frontiers in Physics, 2020, 8, .	2.1	14
118	There is a world beyond αvβ3-integrin: Multimeric ligands for imaging of the integrin subtypes αvβ6, αvβ8, αvÎ and α5β1 by positron emission tomography. EJNMMI Research, 2021, 11, 106.	² 3, 2.5	14
119	Deep Neural Networks and Machine Learning Radiomics Modelling for Prediction of Relapse in Mantle Cell Lymphoma. Cancers, 2022, 14, 2008.	3.7	14
120	A Case of Multimodality Multiparametric 11C-Choline PET/MR for Biopsy Targeting in Prior Biopsy-Negative Primary Prostate Cancer. Clinical Nuclear Medicine, 2012, 37, 918-919.	1.3	13
121	Multimodality Multiparametric Imaging of Early Tumor Response to a Novel Antiangiogenic Therapy Based on Anticalins. PLoS ONE, 2014, 9, e94972.	2.5	13
122	Diagnostic accuracy of intraoperative perfusion-weighted MRI and 5-aminolevulinic acid in relation to contrast-enhanced intraoperative MRI and 11C-methionine positron emission tomography in resection of glioblastoma: a prospective study. Neurosurgical Review, 2019, 42, 471-479.	2.4	13
123	Effect of Tumor Perfusion and Receptor Density on Tumor Control Probability in ¹⁷⁷ Lu-DOTATATE Therapy: An In Silico Analysis for Standard and Optimized Treatment. Journal of Nuclear Medicine, 2021, 62, 92-98.	5.0	13
124	Three-dimensional Magnetic Resonance Imaging Using Single Breath-hold k-t BLAST for Assessment of Global Left Ventricular Functional Parameters. Academic Radiology, 2013, 20, 987-994.	2.5	11
125	Data driven diagnostic classification in Alzheimer's disease based on different reference regions for normalization of PiB-PET images and correlation with CSF concentrations of Al² species. NeuroImage: Clinical, 2018, 20, 603-610.	2.7	11
126	Technical Note: Optimal sampling schedules for kidney dosimetry based on the hybrid planar/SPECT method in 177 Luâ€PSMA therapy. Medical Physics, 2019, 46, 5861-5866.	3.0	11

#	Article	IF	CITATIONS
127	Quantitative DWI predicts event-free survival in children with neuroblastic tumours: preliminary findings from a retrospective cohort study. European Radiology Experimental, 2019, 3, 6.	3.4	10
128	A simulation-based method to determine optimal sampling schedules for dosimetry in radioligand therapy. Zeitschrift Fur Medizinische Physik, 2019, 29, 314-325.	1.5	10
129	Important pharmacokinetic parameters for individualization of ¹⁷⁷ Luâ€PSMA therapy: A global sensitivity analysis for a physiologicallyâ€based pharmacokinetic model. Medical Physics, 2021, 48, 556-568.	3.0	10
130	Comparison of Quantification of Target-Specific Accumulation of [18F]F-siPSMA-14 in the HET-CAM Model and in Mice Using PET/MRI. Cancers, 2021, 13, 4007.	3.7	10
131	A population-based method to determine the time-integrated activity in molecular radiotherapy. EJNMMI Physics, 2021, 8, 82.	2.7	10
132	Current Staging Procedures in Urinary Bladder Cancer. Diagnostics, 2013, 3, 315-324.	2.6	9
133	Combining Computed Tomography and Histology Leads to an Evolutionary Concept of Hepatic Alveolar Echinococcosis. Pathogens, 2020, 9, 634.	2.8	9
134	A Physiologically Based Pharmacokinetic Model for In Vivo Alpha Particle Generators Targeting Neuroendocrine Tumors in Mice. Pharmaceutics, 2021, 13, 2132.	4.5	9
135	Imaging of angiogenesis: from morphology to molecules and from bench to bedside. European Journal of Nuclear Medicine and Molecular Imaging, 2010, 37, 1-3.	6.4	8
136	Limited-projection-angle hybrid fluorescence molecular tomography of multiple molecules. Journal of Biomedical Optics, 2014, 19, 046016.	2.6	8
137	Drug-induced cerebral glucose metabolism resembling Alzheimer's Disease: a case study. BMC Psychiatry, 2015, 15, 157.	2.6	8
138	18F-fluorothymidine PET for predicting survival in patients with resectable pancreatic cancer. Oncotarget, 2018, 9, 10128-10134.	1.8	8
139	Clinicoanatomical substrates of selfish behaviour in amyotrophic lateral sclerosis – An observational cohort study. Cortex, 2022, 146, 261-270.	2.4	8
140	Combination therapy with brentuximab vedotin and cisplatin/cytarabine in a patient with primarily refractory anaplastic lymphoma kinase positive anaplastic large cell lymphoma. OncoTargets and Therapy, 2014, 7, 1123.	2.0	7
141	Response Evaluation in Head and Neck Oncology: Definition and Prediction. Orl, 2017, 79, 14-23.	1.1	7
142	Changes of Radiation Treatment Concept Based on 68Ga-PSMA-11-PET/CT in Early PSA-Recurrences After Radical Prostatectomy. Frontiers in Oncology, 2021, 11, 665304.	2.8	7
143	Quantitative analysis of regional distribution of tau pathology with 11C-PBB3-PET in a clinical setting. PLoS ONE, 2022, 17, e0266906.	2.5	7
144	Population-Based Modeling Improves Treatment Planning Before 90Y-Labeled Anti-CD66 Antibody Radioimmunotherapy. Cancer Biotherapy and Radiopharmaceuticals, 2015, 30, 285-290.	1.0	6

#	Article	IF	CITATIONS
145	Modelling the internalisation process of prostate cancer cells for PSMA-specific ligands. Nuclear Medicine and Biology, 2019, 72-73, 20-25.	0.6	6
146	Multimodal Tumor Therapy in a 31-Year-Old Pregnant Woman with Wilms Tumor. Urologia Internationalis, 2009, 83, 364-367.	1.3	5
147	Mathematical Modeling of In Vivo Alpha Particle Generators and Chelator Stability. Cancer Biotherapy and Radiopharmaceuticals, 2021, , .	1.0	5
148	PET imaging with 68Gallium-labelled ligand of prostate-specific membrane antigen (68Ga-HBED-PSMA) for staging of biochemical recurrent prostate cancer after radical prostatectomy Journal of Clinical Oncology, 2015, 33, 5023-5023.	1.6	5
149	PET/CT for the diagnosis, staging and restaging of prostate cancer. Imaging in Medicine, 2011, 3, 571-585.	0.0	4
150	Inversion-recovery single-shot cardiac MRI for the assessment of myocardial infarction at 1.5 T with a dedicated cardiac coil. British Journal of Radiology, 2012, 85, e709-e715.	2.2	4
151	Double-strand breaks in lymphocyte DNA of humans exposed to [18F]fluorodeoxyglucose and the static magnetic field in PET/MRI. EJNMMI Research, 2020, 10, 43.	2.5	4
152	FDG PET correlates weakly with HIF-1 α expression in solid tumors: a meta-analysis. Acta Radiologica, 2021, 62, 557-564.	1.1	4
153	Quantitation of the In-Mouth Release of Heteroatomic Odorants. ACS Symposium Series, 2002, , 296-311.	0.5	3
154	Magnetic resonance colonography: A promising new technique. Current Gastroenterology Reports, 2004, 6, 389-394.	2.5	3
155	[111In]DOTATOC as a dosimetric substitute for kidney dosimetry during [90Y]DOTATOC therapy: results and evaluation of a combined gamma camera/probe approach. European Journal of Nuclear Medicine and Molecular Imaging, 2006, 33, 1328-1336.	6.4	3
156	Alternative PET Tracers in Musculoskeletal Disease. PET Clinics, 2010, 5, 363-374.	3.0	3
157	PET imaging with of prostate-specific membrane antigen (PSMA) for staging of primary prostate cancer with 68Ca-HBED-PSMA Journal of Clinical Oncology, 2015, 33, e16038-e16038.	1.6	3
158	[68Ga]Pentixafor: A Novel PET Tracer for Imaging CXCR4 Status in Patients with Multiple Myeloma. Blood, 2014, 124, 2014-2014.	1.4	3
159	Pancreatic and Hepatobiliary Cancers. Methods in Molecular Biology, 2011, 727, 243-264.	0.9	2
160	MP42-08 STAGING OF INTERMEDIATE AND HIGH-RISK PROSTATE CANCER USING WHOLE BODY 68GALLIUM-LABELLED LIGAND OF PROSTATE-SPECIFIC MEMBRANE ANTIGEN PET/MRI. Journal of Urology, 2014, 191, .	0.4	2
161	Editorial European Journal of Nuclear Medicine and Molecular Imaging. European Journal of Nuclear Medicine and Molecular Imaging, 2017, 44, 284-285.	6.4	2
162	Multiparametric 18F–FDG PET/MR follow-up in a patient with autoimmune pancreatitis. European Journal of Hybrid Imaging, 2017, 1, 11.	1.5	2

#	Article	IF	CITATIONS
163	Computed Tomography-Based Tumor Heterogeneity Analysis Reveals Differences in a Cohort with Advanced Pancreatic Carcinoma under Palliative Chemotherapy. Visceral Medicine, 2021, 37, 77-83.	1.3	2
164	A Whole-Body Physiologically Based Pharmacokinetic Model for Alpha Particle Emitting Bismuth in Rats. Cancer Biotherapy and Radiopharmaceuticals, 2021, , .	1.0	2
165	Value of PET imaging for radiation therapy. Nuklearmedizin - NuclearMedicine, 2021, 60, 326-343.	0.7	2
166	2388. International Journal of Radiation Oncology Biology Physics, 2006, 66, S425-S426.	0.8	1
167	Demonstration of metastatic tumour growth following vessel structures by PET/CT. European Journal of Nuclear Medicine and Molecular Imaging, 2009, 36, 1021-1021.	6.4	1
168	Kidney, Urinary Tract, and Bladder. , 2016, , 875-915.		1
169	Can Met-PET/CT Predict Sporadic Multiglandular Hyperparathyroidism? Report of a Case and Review of the Literature. Case Reports in Endocrinology, 2019, 2019, 1-4.	0.4	1
170	Tumor Vasculature. , 2021, , 831-867.		1
171	Comparison of MRI-based and PET-based image pre-processing for quantification of 11C-PBB3 uptake in human brain. Zeitschrift Fur Medizinische Physik, 2021, 31, 37-47.	1.5	1
172	An in silico study on the effect of the radionuclide half-life on PET/CT imaging with PSMA-targeting radioligands. Nuklearmedizin - NuclearMedicine, 2021, 60, 33-37.	0.7	1
173	18F-FDG-PET/MR in Alveolar Echinococcosis: Multiparametric Imaging in a Real-World Setting. Pathogens, 2022, 11, 348.	2.8	1
174	MP42-18 IMAGING OF RECURRENT PROSTATE CANCER USING 68GALLIUM-LABELLED LIGAND OF PROSTATE-SPECIFIC MEMBRANE ANTIGEN PET/CT AND PET/MRI. Journal of Urology, 2014, 191, .	0.4	0
175	PD32-06 DETECTION RATES OF 68GALLIUM-LABELLED LIGAND OF PSMA PET/CT AND PET/MRI IN 332 CONSECUTIVE PATIENTS WITH BIOCHEMICAL RECURRENCY AFTER RADICAL PROSTATECTOMY. Journal of Urology, 2015, 193, .	0.4	0
176	Workflow and Protocol Considerations. , 2018, , 151-168.		0
177	Impact of rs12917 MGMT Polymorphism on [18F]FDG-PET Response in Pediatric Hodgkin Lymphoma (PHL). Molecular Imaging and Biology, 2019, 21, 1182-1191.	2.6	0
178	Molecular Imaging of Angiogenesis. , 2010, , 105-115.		0
179	Changes in the tumor glucose-uptake measured by 18F-FDG PET with two weeks of single-agent cetuximab in localized squamous cell carcinoma of the esophagus Journal of Clinical Oncology, 2013, 31, e15042-e15042.	1.6	0